Dona AA, Sanchez JF, Palmer JM, Synold TW, Chiuppesi F, Thomas S, Caserta E, Singer M, Tandoh T, Chowdhury A, Krishnan A, Rosenzweig M, Diamond DJ, Rosen S, Pichiorri F, Dadwal S. Leflunomide Confers Rapid Recovery from COVID-19 and is Coupled with Temporal Immunologic Changes. J Immunological Sci. (2023); 7(1): 9-27

Journal of Immunological Sciences

Case Report Open Access

Leflunomide Confers Rapid Recovery from COVID-19 and is Coupled with Temporal Immunologic Changes

Ada Alice Dona[1,2#], James F Sanchez[1#], Joycelynne M Palmer[3], Timothy W. Synold[4], Flavia Chiuppesi[5], Sandra Thomas[2], Enrico Caserta[1,2], Mahmoud Singer[1,2], Theophilus Tandoh[1,2], Arnab Chowdhury[3], Amrita Krishnan[1], Michael Rosenzweig[1], Don J Diamond[5], Steven Rosen[1*], Flavia Pichiorri[1,2*], Sanjeet Dadwal[6*]

[1]Judy and Bernard Briskin Center for Multiple Myeloma Research, Department of Hematology and Hematopoietic Cell Transplantation, City of Hope, Duarte, CA
[2]Department of Hematologic Malignancies Translational Science, Beckman Research Institute, City of Hope, Duarte, CA
[3]Department of Computational and Quantitative Sciences, Beckman Research Institute, City of Hope, Duarte, CA
[4]Department of Cancer Biology, City of Hope, Duarte, CA
[5]Department of Experimental Therapeutics, City of Hope, Duarte, CA
[6]Department of Medicine, Division of Infectious Disease, City of Hope, Duarte, CA USA
[#]These authors contributed equally to this work.

Article Info

Article Notes
Received: October 21, 2022
Accepted: January 20, 2023

***Correspondence:**

*Corresponding Authors:

[1]Steven Rosen, Judy and Bernard Briskin Center for Multiple Myeloma Research, Department of Hematology and Hematopoietic Cell Transplantation, City of Hope, Duarte, CA; Email: srosen@coh,org.

[2]Sanjeet Dadwal, Department of Medicine, Division of Infectious Disease, City of Hope, Duarte, CA, USA; Email: sdadwal@coh.org

[3]Flavia Pichiorri, Judy and Bernard Briskin Center for Multiple Myeloma Research, Department of Hematology and Hematopoietic Cell Transplantation, City of Hope, Duarte, CA; Email: fpichiorri@coh.org.

Keywords
Leflunomide
COVID-19
Breast cancer
Clinical trial
Drug repurposing

ABSTRACT

Background: Vaccines for SARS-CoV-2 have been considerably effective in reducing rates of infection and severe COVID-19. However, many patients, especially those who are immunocompromised due to cancer or other factors, as well as individuals who are unable to receive vaccines or are in resource-poor countries, will continue to be at risk for COVID-19. We describe clinical, therapeutic, and immunologic correlatives in two patients with cancer and severe COVID-19 who were treated with leflunomide after failing to respond to standard-of-care comprising remdesivir and dexamethasone. Both patients had breast cancer and were on therapy for the malignancy.

Methods: The protocol is designed with the primary objective to assess the safety and tolerability of leflunomide in treating severe COVID-19 in patients with cancer. Leflunomide dosing consisted of a loading dose of 100 mg daily for the first three days, followed by daily dosing, at the assigned dose level (Dose Level 1: 40 mg, Dose Level -1, 20 mg; Dose Level 2, 60 mg), for an additional 11 days. At defined intervals, serial monitoring of blood samples for toxicity, pharmacokinetics, and immunologic correlative studies were performed, as well as nasopharyngeal swabs for PCR analysis of SARS-CoV-2.

Results: Preclinically, leflunomide impaired viral RNA replication, and clinically, it led to a rapid improvement in the two patients discussed herein. Both patients completely recovered, with minimal toxicities; all adverse events experienced were considered unrelated to leflunomide. Single-cell mass-cytometry analysis showed that leflunomide increased levels of CD8+ cytotoxic and terminal effector T cells and decreased naïve and memory B cells.

Conclusions: With ongoing COVID-19 transmission and occurrence of breakthrough infections in vaccinated individuals, including patients with cancer, therapeutic agents that target both the virus and host inflammatory response would be helpful despite the availability of currently approved anti-viral agents. Furthermore, from an access to care perspective, especially in resource-limited areas, an inexpensive, readily available, effective drug with existing safety data in humans is relevant in the real-world setting

Background

Vaccines for SARS-CoV-2, the causative agent of COVID-19, have been considerably effective in reducing rates of infection and severe COVID-19. However, many individuals, including some patients with cancer, people who are unable to receive vaccines, or individuals in resource-poor countries, where access to antiviral medications,

monoclonal antibodies, and vaccines is limited, will continue to be at risk for COVID-19. In infected patients, the non-specific innate immune response is followed by adaptive immunity mediated by both B cells and T cells,[1] but patients with cancer and other disorders may be impacted by a dysregulated immune response.

Leflunomide is an FDA-approved, oral agent that has been commercially available since 1998. It is used for the treatment of rheumatoid arthritis as a single agent or in combination with methotrexate. Its primary mechanism of action is inhibiting *de novo* pyrimidine synthesis by targeting dihydroorotate dehydrogenase (DHODH)[2], with an anti-proliferative effect in B- and T-lymphocytes[3]. Teriflunomide is the active primary metabolite of leflunomide.

Host-targeting antiviral drugs may be appealing by targeting the host machinery exploited by the virus, thereby potentially applying to a wide range of viruses and viral strains. To this end, repurposed drugs are especially suitable, as many of the extensive preclinical validation and toxicity studies have already been performed. As a DHODH inhibitor, leflunomide is worthy of study for SARS-CoV-2, an RNA virus, particularly because of the virus's high content of uracil[4], one of the two nucleobases inhibited by leflunomide. Leflunomide has been used in difficult-to-treat cytomegalovirus infections in patients undergoing hematopoietic cell transplantation and in polyoma virus (BK virus) hemorrhagic cystitis when no alternatives are available.

Methods

The protocol is designed as a phase 1/ 2 trial with the primary objective to assess the safety and tolerability of leflunomide in treating severe COVID-19 in patients with cancer (NCT04532372). The study was performed in accordance with the provisions of the Declaration of Helsinki and approved by the City of Hope Institutional Review Board. All participants gave written informed consent. Leflunomide dosing comprised a loading dose of 100 mg daily for the first three days, followed by daily dosing at the assigned dose level (Dose Level 1: 40 mg, Dose Level -1, 20 mg; Dose Level 2, 60 mg), for an additional 11 days. At defined intervals, serial monitoring of blood samples for toxicity, pharmacokinetics, and immunologic correlative studies were performed, as well as nasopharyngeal swabs for PCR analysis of SARS-CoV-2.

Primary Samples

Biospecimen collection and immunological analyses are detailed below. Briefly, peripheral blood from healthy donors was obtained from the institutional hematopoietic tissue repository. Specifically, the cellular fraction of the peripheral blood mononuclear cells (PBMCs) was isolated using Ficoll-Paque Plus (GE Healthcare, Life Science) following the manufacturer's instructions.

Mass Cytometry (CyTOF) Staining and Acquisition

A total of 2-4x10^6 PBMCs were stained with a panel containing 30 metal-conjugated antibodies (**Sup. Table 1**) according to Fluidigm's protocol for Maxpar Antibody Labeling (PRD002 Rev 12). PBMCs derived from the clinical trial were stained with Fluidigm's Maxpar Direct Immune Profiling Assay Cell Staining (PN 400286 B1). Samples were acquired, exported as FCS files, and normalized on Fluidigm's Helios (Software 7.0.5189).

CyTOF Analysis

Non-custom panel analysis was analyzed using Maxpar Pathsetter™ software powered by GemStone 2.0.41, Verity Software House, Topsham, Maine (Version 2.0.45). The FCS files were also analyzed using FlowJo™ Software (Windows edition, Version 10.6. Becton Dickinson Company; 2019), and the Cytobank© platform (https://www.cytobank.org) (Cytobank, Inc., Mountain View, CA) was used for gating, tSNE plotting, and FlowSOM.

Pharmacokinetic Analysis

Pharmacokinetic sampling was performed per protocol during active treatment with leflunomide. Samples were collected prior to initiation of drug administration, daily for days +1 to +7 of treatment, and subsequently daily if the subject was hospitalized, or during visits if the subject was outpatient. Plasma was analyzed for total (bound and unbound) and free (unbound) teriflunomide concentrations using a previously described LC-MS/MS method[5]. Briefly, following addition of a deuterated teriflunomide internal standard, plasma (total drug) or ultrafiltered plasma (free drug) samples were prepared by protein precipitation using 3:1 ice cold methanol. The resulting protein-free plasma or ultrafiltered plasma was further diluted 10,000-fold with 0.5 mM ammonium acetate, 0.025% formic acid in 75% methanol, and 10 µl was injected for analysis. The lower limits of quantitation of the assay were 30 µg/ml and 30 ng/ml in plasma and ultrafiltered plasma, respectively.

DLT Definitions

Dose limiting toxicity (DLT) was defined as any of the following toxicities that were at least possibly related to leflunomide:

- Hematologic DLT events (any adverse events [AEs] considered at least possibly attributable to study treatment):
  - For patients with *solid tumor malignancies*, all grade 3 or 4 hematologic AEs
  - For patients with *hematologic malignancies*, the following AEs would be considered DLTs if they were determined as not attributable to underlying hematological malignancy.

- Grade 4 neutropenia (absolute neutrophil count [ANC] <500/mm^3)
- Grade 3 or 4 febrile neutropenia
- Grade 4 thrombocytopenia (<25,000/mm^3)
- Grade 3 thrombocytopenia (<50,000/mm^3) with bleeding

• Non-Hematologic AEs (any treatment emergent AEs):

o ≥ Grade 3 non-hematologic toxicity excepting the following:

- Alopecia
- Grade 3 nausea/vomiting/diarrhea for less than 72 hours treated with adequate antiemetic and other supportive care
- Grade 3 fatigue for < 1 week
- ≥ Grade 3 electrolyte abnormalities that are not clinically complicated and resolve spontaneously or to conventional medical interventions within 72 hours
- ≥ Grade 3 amylase or lipase elevation not associated with symptoms or clinical manifestations of pancreatitis

o Treatment-emergent increase in serum ALT or AST to > 3x ULN associated with an increase in serum total bilirubin to > 2x ULN (consistent with Hy's Law).

• Any treatment-emergent Grade 5 AE that occurs during the 28-day treatment period that is not due to underlying malignancy would be considered a DLT.

Cholestyramine

Leflunomide is reabsorbed from the gastrointestinal tract and consequently is detectable in the body for up to 2 years. Cholestyramine, a bile acid sequestrant, fixes the metabolite, preventing reabsorption and expediting drug elimination. We administered cholestyramine daily starting on day 29 until plasma levels of teriflunomide were less than 0.02 mg/L by two separate measurements 14 days apart.

Cell culture

Multiple myeloma (MM) cell lines MM.1S and U266 were purchased from ATCC. All cell lines were cultured in RPMI-1640 medium supplemented with 10% fetal bovine serum (FBS) (Cat. #019K8420, Sigma), 100 IU/mL penicillin, and 100 µg/mL streptomycin (Cat.#15140-122, Gibco).

Immunoblotting

Cells lyses in RIPA buffer (89901, Thermo Scientific) were supplemented with protease and phosphatase inhibitors, and then sonicated (30" Pulse ON 02" Pulse OFF 03" 60% amplification). Lysates were then clarified by spinning at 14,000 rpm at 4°C and protein concentration quantified by BCA Protein Assay (23227, Thermo Scientific). Forty micrograms of proteins were denatured in boiling SDS sample buffer, resolved on 4%-20% gradient gels (Cat.# 5671093, Bio-Rad), and transferred to nitrocellulose membranes (Cat.# 1704271 Bio-Rad). After blocking nonspecific binding of antibody with 5% BSA (Fisher BioReagents), blots were probed with anti-RV σ-NS (1:1000; provided by Oncolytics Biotech Inc.) to assess viral replication for σ1 protein, or GAPDH (Cat.# sc-32233, Santa Cruz Biotechnology) as internal control. Blots were washed three times for 15 minutes with TBST 1X and stained with horseradish peroxidase (HRP)-conjugated secondary antibodies (diluted 1:4000) for 2hrs at room temperature. Primary antibodies were detected by binding with secondary antibodies donkey anti-goat IgG (H+L) (Cat.# A16005, Invitrogen) and goat anti-mouse IgG-HRP (NA931, GE Healthcare), and using an enhanced chemiluminescent visualization system (Cat.#RPN2209 ECL Western Blotting Detection Reagents, GE Healthcare). Primary and secondary antibodies were diluted according to the manufacturer instructions. The bands were quantified by densitometry analyses using Image Lab program (Biorad) and normalized to GAPDH.

RNA isolation and analysis

Total cellular RNA was extracted by using TRIZOL reagent (Cat. #15596018 Invitrogen Corporation) and RNA Clean-Up and Concentration Kit (Cat. #43200 Norgen) according to the manufacturer's protocols. cDNA synthesis was performed by using the High Capacity cDNA Reverse Transcription Kit (Applied Biosystems, Cat# 4368814). Reverse transcription reactions were run using a Mastercycler pro. Quantitative real time-PCR (qRT-PCR) was performed with the TaqMan method (Applied Biosystems), according to the manufacturer's instructions. The appropriate TaqMan probes for mRNA quantification were purchased from Applied Biosystems, and all reactions were performed in triplicate. The following probes were used: (HS99999905_m1) GAPDH used as endogenous control; (HS00989291_m1) INF-γ; (Hs00961622 m1) IL-10; (Hs00174131 m1) IL-6; (Hs01077958 S1) IFNB1; (Hs00174128 m1) TNFalpha; (Hs00265051 S1) IFNA2.

For the quantification of viral RNA of genomes extracted from infected PBMCs from healthy donors and MM cell lines, q-RT-PCR reactions were conducted using the PowerUp SYBR Green Master Mix (Applied Biosystems Cat.# 4367659) according to the manufacturer's instructions and the following primers: Reo9: 5′-TG CGC AAG AGG CAG CAA TCG-3′ and Reo10: 5′-TT CGC GGG CCT CGC ACA TTC-3′; GAPDH FD: 5′- CTG CAC CAC CAA CTG CTT -3′ and GAPDH RV: 5′- CAT GAC GGC AGG TCA GGT -3′.

Cytokine measurements

Samples were analyzed for 30 cytokines using the Human Cytokine Thirty-Plex Antibody Magnetic Bead Kit (Invitrogen, Camarillo, CA) as per the manufacturer's protocol. Briefly, Invitrogen's multiplex bead solution was vortexed for 30 seconds, and 25 µl was added to each well of a flat-bottom 96 well microplate. Samples (e.g., plasma) were diluted 1:2 with assay diluent and loaded into the wells containing 50 µl of incubation buffer. Cytokine standards were reconstituted with assay diluent, and serial dilutions of cytokine standards were prepared in parallel and added to the plate. Plates were incubated on a shaker at 500 rpm in the dark at room temperature for 2 hours. The plate was then applied to a magnetic capture device and washed three times with 200 µl of wash buffer. After the final wash, 200 µl of a biotinylated detection antibody mixture was added to each well, and the plate was incubated on a shaker for 1 hour. After washing again three times with 200 µl of wash buffer, streptavidin-phycoerythrin (100 µl) was added to the wells. The plate was incubated on a plate shaker for another 30 minutes and washed three times, after which the beads were resuspended in 150 µl of wash buffer and shaken for 1 minute. Finally, the assay plate was transferred to a Flexmap 3D Luminex system (Luminex Corp, Austin, TX) for analysis. Cytokine concentrations were calculated using Bio-Plex Manager 6.0 software with a five parameter curve-fitting algorithm applied for standard curve calculations for duplicate samples.

Results and Discussion

Previous data have demonstrated the preclinical anti-viral activity of DHODH inhibitors against RNA viruses such as influenza, Ebola, and Zika viruses, as well as SARS-CoV-2[6]. In support of the importance of DHODH in viral replication, viral growth was largely inhibited in DHODH knockout cells, and addition of uracil and cytosine (the pyrimidine bases) restored viral activity[6].

Reovirus serotype 3–dearing strain (RV) is a naturally occurring, ubiquitous, nonenveloped human reovirus with a genome that consists of 10 segments of double-stranded RNA. As with SARS-CoV-2, RV can infect human and animals and never passes through a DNA phase. It actively replicates its RNA genome and induces a strong anti-viral immune response. The two viruses primarily differ in the composition of the envelope and the fact that coronaviruses need to synthetize the RNA negative strand before initiating transcription. Our preliminary data show that leflunomide significantly arrested RV productive infection in cancer cells, as shown by decreased capsid formation and genome replication **(Sup. Fig. 1A-F)**. Impairment in viral replication was also observed when PBMCs were treated with teriflunomide, the active metabolite of leflunomide, in combination with RV, compared to the virus alone **(Sup. Fig. 1G-H)**. Our data also show that, in the ex vivo setting, the addition of teriflunomide to RV-infected PBMCs significantly decreased the expression of highly inflammatory cytokines such as IL-6 and GM-CSF **(Sup. Fig. 1I-J)** but concomitantly enhanced the anti-viral interferon I (IFN-α and IFN-β) response and TNF-α **(Sup. Fig. 1K-L-M)**. The antiviral activity of leflunomide aligns with the experience of the drug as an agent against cytomegalovirus (CMV) and polyoma BK virus infections in immunocompromised hosts[7,8].

We furthermore describe our findings of two patients with breast cancer who were admitted to our COVID unit after worsening shortness of breath due to COVID-19. Both patients' oxygen levels decreased to below 90%, requiring high-flow oxygen. Computed tomography (CT) of the chest revealed multifocal pneumonia in both patients **(Fig. 1A-B)**. The patients began treatment with remdesivir, dexamethasone, cefepime, and azithromycin, with minimal improvement. No co-infections were identified, and the clinical condition was due to COVID-19.

We administered leflunomide to both patients following informed consent and confirmation of eligibility to participate in the clinical trial. After loading with leflunomide with a dose of 100 mg daily x 3 days, the patients received 40 mg daily for 11 additional days. Leflunomide is reabsorbed from the gastrointestinal tract and consequently is detectable in the body for up to 2 years. Cholestyramine, a bile acid sequestrant, fixes the metabolite, preventing reabsorption and expediting drug elimination. We administered cholestyramine daily starting on day 29 until plasma levels of teriflunomide were less than 0.02 mg/L by two separate measurements 14 days apart. Plasma concentrations of teriflunomide were also measured throughout the treatment period in both patients as previously described[9]. Maximum plasma concentrations (Cmax) achieved in the two subjects were 252.4 and 152.3 µmol/L, respectively, and the areas-under-the-curve (AUC) were 5598.0 and 3498.1 µmol/L x day. As shown in the concentration-versus-time plots (**Sup. Fig. 2A**), plasma concentrations were maintained above the in vitro EC_{50} against SARS-CoV-2 (26 µmol/L) [6] for >36 days.

The patients had rapid improvement in symptoms and oxygenation and experienced a complete recovery as clearly shown from the CT scans of the lung before and after combination therapy that included leflunomide **(Fig. 1A-B)**. The adverse events that were observed were minimal and considered unrelated to leflunomide. These findings are consistent with a pilot study in which 15 patients given leflunomide had improved viral clearance and hospital discharge rate when compared to 12 patients in a control arm[10]. Because leflunomide is an immune suppressive drug, which could potentially impair its anti-viral activity, we decided to follow the immune changes of these patients

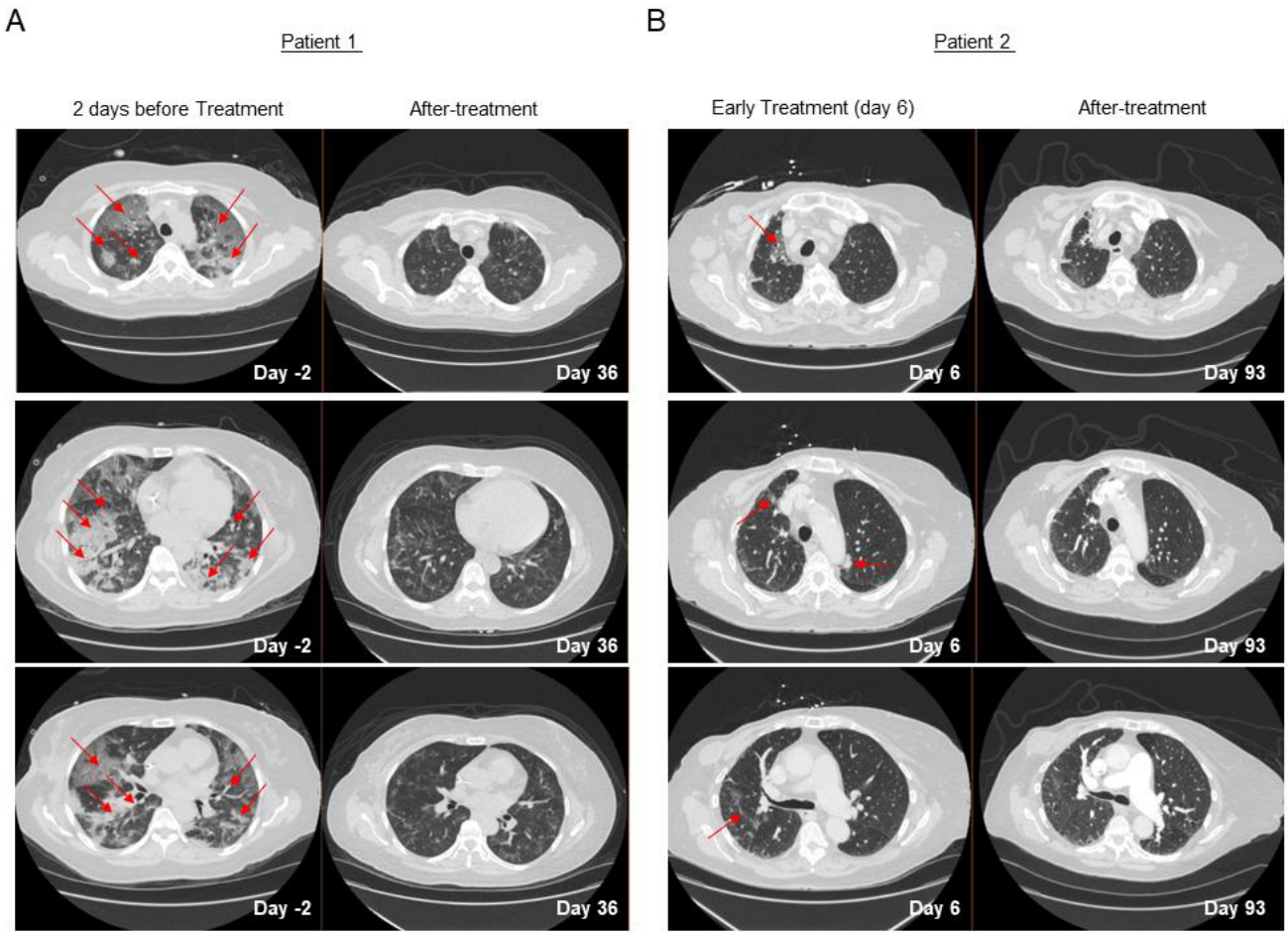

Figure 1: A-B) Serial CT chest scans from patient 1 (A) and 2 (B) with severe COVID-19 pneumonia showing peripheral multilobar ground glass opacities (red arrow) two days before the initiation of leflunomide treatment for patient 1 and Day 6 of treatment for patient 2. Scans obtained after 36 days (A) and after 93 days (B) on treatment show partial absorption of the abnormalities for both patients

during and after the course of treatment. A 30-marker single cell mass cytometry (CyTOF) antibody panel **(Sup. Table 1)** designed to identify twenty different immune compartments **(Sup. Table 2)** was used to perform a longitudinal high dimensional immune profiling **(Fig. 2A and Sup. Fig. 2B-C)**.

In both patients, we observed a substantial decrease in the total number of B cells following leflunomide treatment **(Fig. 2B and Sup. Fig. 2D) (Sup. Tables 3 and 4)**. This finding is consistent with the regulatory activity of leflunomide on B cell proliferation that was previously observed in animals[11]. Although leflunomide has been considered an immunosuppressive drug by inhibiting cellular and humoral mediated responses[12], in both patients, we observed a robust expansion in CD8+ cytotoxic T cells after 5 days from the initial dosing. This effect further increased upon subsequent doses, reaching maximum expansion at around 21 days after the initial treatment **(Fig. 2C and Sup. Fig. 2E-G)**. Among the CD8+ cytotoxic T cells, the major increase was observed in the effector memory (EM) and in the CD45RA+ terminal effector T cell population (TEMRA CD8+) **(Fig. 2D)**, whereas the other T cell populations, including naïve and central memory (CM), were nearly unaffected. These data are wholly aligned with recently published data[13] showing that expansion of CD8+ cytotoxic T cells, including long lived, antigen-experienced T cells (CD45RA+), contribute to SARS-CoV-2 recovery in cancer patients. Intriguingly, in three patients with relapsed multiple myeloma enrolled in our single agent leflunomide phase 1 trial[9], we observed that leflunomide elicited the same immune stimulatory effect on CD8+ cytotoxic T cells (unpublished data), further supporting an unexpected immune stimulatory role of this agent in cancer patients.

Although changes in the percentage of total CD4+ T cells differed among the two patients, both patients showed an increase in CD4+ TEMRA cells, while instead an increase in CM and EM CD4+ T cells was only present in the second patient **(Fig. 2D and Sup. Fig. 2H-J)**.

An increase in pro-inflammatory CD16+ cells, such as intermediate and non-classical monocytes, was additionally

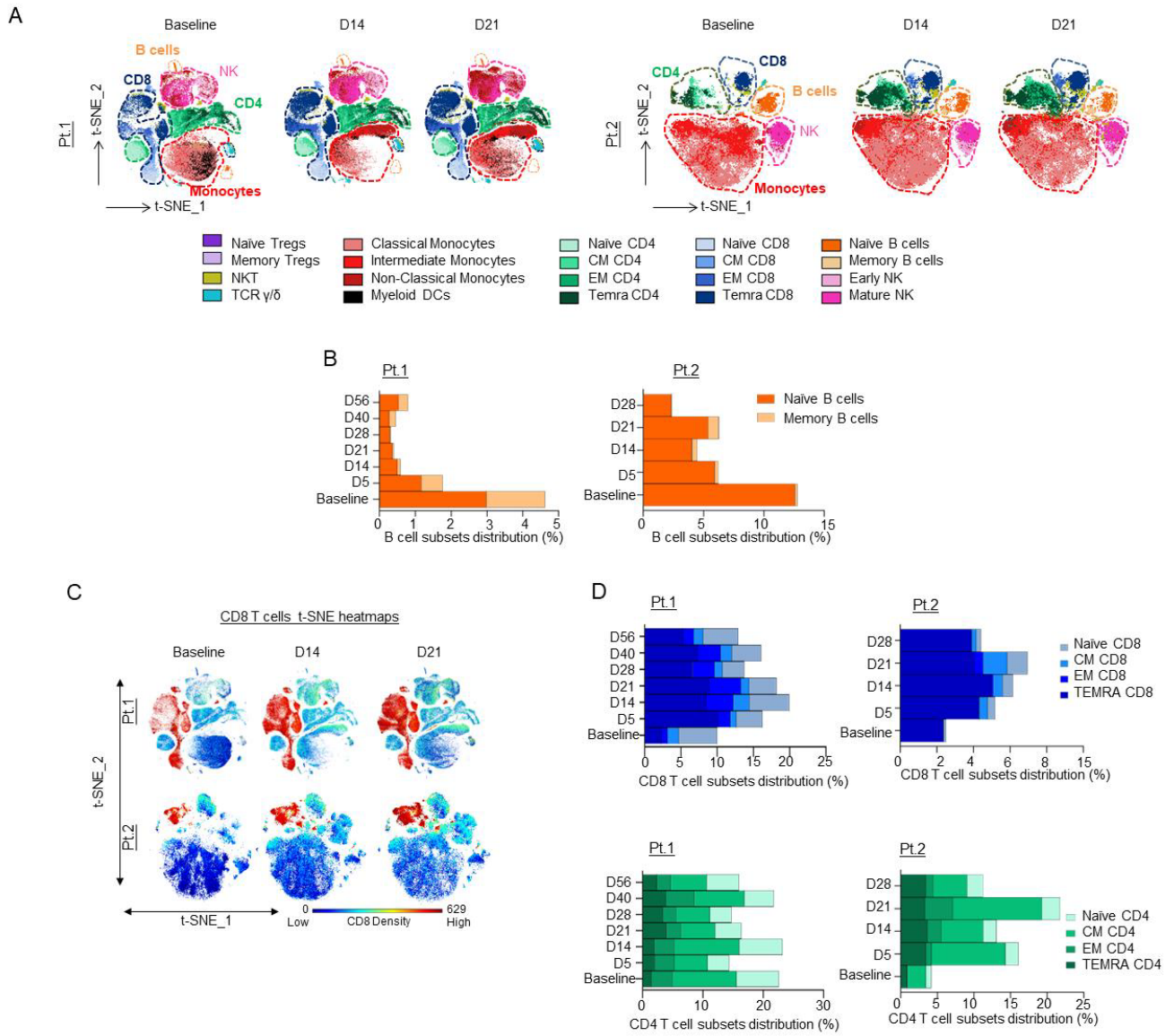

Figure 2: A) In-depth longitudinal immune profiling of two patients with COVID-19 and breast cancer treated with 40 mg leflunomide. A Maxpar Direct Immune Profiling System using a dry 30-marker antibody panel was employed. Hierarchical clustering and statistical mapping were performed algorithmically via the Cytobank© platform. vi-SNE analysis (iterations=1000, perplexity=100) are displayed in 2D plots using the resultant t-SNE 1 and t-SNE 2 dimensions. High-fidelity FlowSOM ("self-organizing map") (metacluster=10 and cluster=100) based on vi-SNE 2D plots showing 20 different immune-compartments was used; **B)** Bar graphs representing the expression of naïve and memory B cell subpopulations through the course of treatment; **C)** t-SNE heatmap highlighting the increased expression of CD8+ cytotoxic T cells at baseline and on days 14 and 21 of treatment in both patients; **D)** Bar graphs showing effector memory and terminally differentiated effector T cells (TEMRA) T cell subsets in percentages compared to the total count PBMCs in both patients.

observed in both patients, but the classical monocyte population remained almost unchanged **(Sup. Fig. 3A-G)**. In line with our observation that leflunomide appears to generally increase anti-viral T cell responses, we also noted a consistent increase among the two patients in total NKT **(Sup. Fig. 3H-I)** and TCR γδ cells **(Sup. Fig. 3J-K),** which play a pivotal role in countering viral infection[14]. A robust increase in the NK cell population, specifically in mature NK cells, over the course of the study was noted in the first patient **(Sup. Fig. 4A-E)**.

Consistent with the decrease in the B cell population, the immunoglobulin profile showed a decrease in total IgM levels in the first patient **(Sup. Fig. 5A)**, an effect that was previously associated with a relatively rapid recovery from COVID-19[15]. This effect was observed seven days after the patient began leflunomide treatment, while total IgG levels remained mostly unchanged **(Sup. Fig. 5B).** A decrease in IgM levels was instead not observed in the second patient **(Sup. Fig. 5C-D)**.

A cytokine array showed that leflunomide treatment

decreased soluble IL2R **(Sup. Fig. 5E-F)**; high levels are regularly associated with inhibition of CD8+ cytotoxic T cells and high rates of hospitalization and mortality[16].

Consistent with previously published data, here we show that leflunomide affects B cell proliferation[17], and for the first time report that leflunomide stimulates anti-viral activity by promoting innate immunity. Our patients treated on a leflunomide protocol had rapid improvements that were coupled with temporal and favorable changes in immunologic response. An important limitation is the small number of patients enrolled to date; however, the data align with two pilot studies comparing leflunomide to leflunomide plus institutional standard of care, one showing that leflunomide plus standard of care conferred favorable SARS-CoV-2 clearance and hospital discharge[10], and the other demonstrating a shorter duration of viral shedding and a reduction in C-reactive protein[18]. A third study assigned patients to either leflunomide or leflunomide plus IFNα and found no statistically significant difference in terms of duration of viral shedding or length of hospital stay[19]. However, the dosing used was lower than in our study, and it is possible that the enhancement of IFNα signaling by leflunomide precludes additional benefit of IFNα intervention. Finally, two separate case series described patients taking teriflunomide for multiple sclerosis who contracted COVID-19 but experienced self-limiting infection[20,21].

Conclusion

We used immunologic correlative experiments to describe the immune response of two patients with severe COVID-19 who were treated with the immune modulator leflunomide. Further study is warranted to more definitely address the effectiveness of leflunomide in the treatment of COVID-19, especially in patients with cancer. Leflunomide treatment might also be relevant for patients who are immunocompromised due to factors other than cancer, but additional evidence is needed. With ongoing COVID-19 transmission, which can overcome precautions such as hand washing and social distancing,[22] and occurrence of breakthrough infections in vaccinated individuals, therapeutic agents that target both the virus and host inflammatory response would be helpful despite the availability of currently approved anti-viral agents. Furthermore, from an access to care perspective, especially in resource-limited areas, an inexpensive, readily available, effective drug with existing safety data in humans is relevant in the real-world setting.

Acknowledgments

We are grateful to the Pathogen & Microbiome Division at TGen North for the sequencing of SARS-CoV-2 strains. The Biostatistics Core at City of Hope was supported by the National Institutes of Health under award number P30CA033572. This research was also in part supported by a P30CA033572 Supplement. The content is solely the responsibility of the authors and does not necessarily represent the official views of the National Institutes of Health. We also acknowledge support from the Norman and Sadie Lee Foundation.

Conflict of Interest

The authors declare that they have no competing interests that are relevant to this study.

References

1. Priyanka, Choudhary OP, Singh I. Protective immunity against COVID-19: Unravelling the evidences for humoral vs. cellular components. Travel Med Infect Dis. 2021; 39: 101911.
2. Davis JP, Cain GA, Pitts WJ, et al. The immunosuppressive metabolite of leflunomide is a potent inhibitor of human dihydroorotate dehydrogenase. Biochemistry. 1996; 35(4): 1270-1273.
3. Baumann P, Mandl-Weber S, Völkl A, et al. Dihydroorotate dehydrogenase inhibitor A771726 (leflunomide) induces apoptosis and diminishes proliferation of multiple myeloma cells. Mol Cancer Ther. 2009; 8(2): 366-375.
4. Romano M, Ruggiero A, Squeglia F, et al. A Structural View of SARS-CoV-2 RNA Replication Machinery: RNA Synthesis, Proofreading and Final Capping. Cells. 2020; 9(5).
5. Parekh JM, Vaghela RN, Sutariya DK, et al. Chromatographic separation and sensitive determination of teriflunomide, an active metabolite of leflunomide in human plasma by liquid chromatography-tandem mass spectrometry. J Chromatogr B Analyt Technol Biomed Life Sci. 2010; 878(24): 2217-2225.
6. Xiong R, Zhang L, Li S, et al. Novel and potent inhibitors targeting DHODH, a rate-limiting enzyme in de novo pyrimidine biosynthesis, are broad-spectrum antiviral against RNA viruses including newly emerged coronavirus SARS-CoV-2. bioRxiv. 2020:2020.2003.2011.983056.
7. Wang E, Jan AS, Doan VP, et al. Leflunomide therapy for refractory cytomegalovirus infections in hematopoietic stem cell transplant recipients. J Oncol Pharm Pract. 2019; 25(7): 1731-1737.
8. Williams JW, Javaid B, Kadambi PV, et al. Leflunomide for polyomavirus type BK nephropathy. N Engl J Med. 2005; 352(11): 1157-1158.
9. Rosenzweig M, Palmer J, Tsai NC, et al. Repurposing leflunomide for relapsed/refractory multiple myeloma: a phase 1 study. Leuk Lymphoma. 2020; 61(7): 1669-1677.
10. Wang Q, Guo H, Li Y, et al. Efficacy and Safety of Leflunomide for Refractory COVID-19: A Pilot Study. Front Pharmacol. 2021; 12: 581833.
11. Siemasko KF, Chong AS, Williams JW, et al. Regulation of B cell function by the immunosuppressive agent leflunomide. Transplantation. 1996; 61(4): 635-642.
12. Breedveld FC, Dayer JM. Leflunomide: mode of action in the treatment of rheumatoid arthritis. Ann Rheum Dis. 2000; 59(11): 841-849.
13. Bange EM, Han NA, Wileyto P, et al. CD8(+) T cells contribute to survival in patients with COVID-19 and hematologic cancer. Nat Med. 2021; 27(7): 1280-1289.
14. Sabbaghi A, Miri SM, Keshavarz M, et al. Role of γδ T cells in controlling viral infections with a focus on influenza virus: implications for designing novel therapeutic approaches. Virol J. 2020; 17(1): 174.
15. Legros V, Denolly S, Vogrig M, et al. A longitudinal study of SARS-CoV-2-infected patients reveals a high correlation between neutralizing antibodies and COVID-19 severity. Cell Mol Immunol. 2021; 18(2): 318-327.

16. Jang HJ, Leem AY, Chung KS, et al. Soluble IL-2R Levels Predict in-Hospital Mortality in COVID-19 Patients with Respiratory Failure. J Clin Med. 2021; 10(18).

17. van der Heijden EH, Hartgring SA, Kruize AA, et al. Additive immunosuppressive effect of leflunomide and hydroxychloroquine supports rationale for combination therapy for Sjögren's syndrome. Expert Rev Clin Immunol. 2019; 15(7): 801-808.

18. Hu K, Wang M, Zhao Y, et al. A Small-Scale Medication of Leflunomide as a Treatment of COVID-19 in an Open-Label Blank-Controlled Clinical Trial. Virologica Sinica. 2020; 35(6): 725-733.

19. Wang M, Zhao Y, Hu W, et al. Treatment of Coronavirus Disease 2019 Patients With Prolonged Postsymptomatic Viral Shedding With Leflunomide: A Single-center Randomized Controlled Clinical Trial. Clinical Infectious Diseases. 2020; 73(11): e4012-e4019.

20. Maghzi AH, Houtchens MK, Preziosa P, et al. COVID-19 in teriflunomide-treated patients with multiple sclerosis. Journal of Neurology. 2020; 267(10): 2790-2796.

21. Mantero V, Baroncini D, Balgera R, et al. Mild COVID-19 infection in a group of teriflunomide-treated patients with multiple sclerosis. Journal of Neurology. 2021; 268(6): 2029-2030.

22. Priyanka, Choudhary OP, Singh I, et al. Aerosol transmission of SARS-CoV-2: The unresolved paradox. Travel Med Infect Dis. 2020; 37: 101869.

Supplementary Files

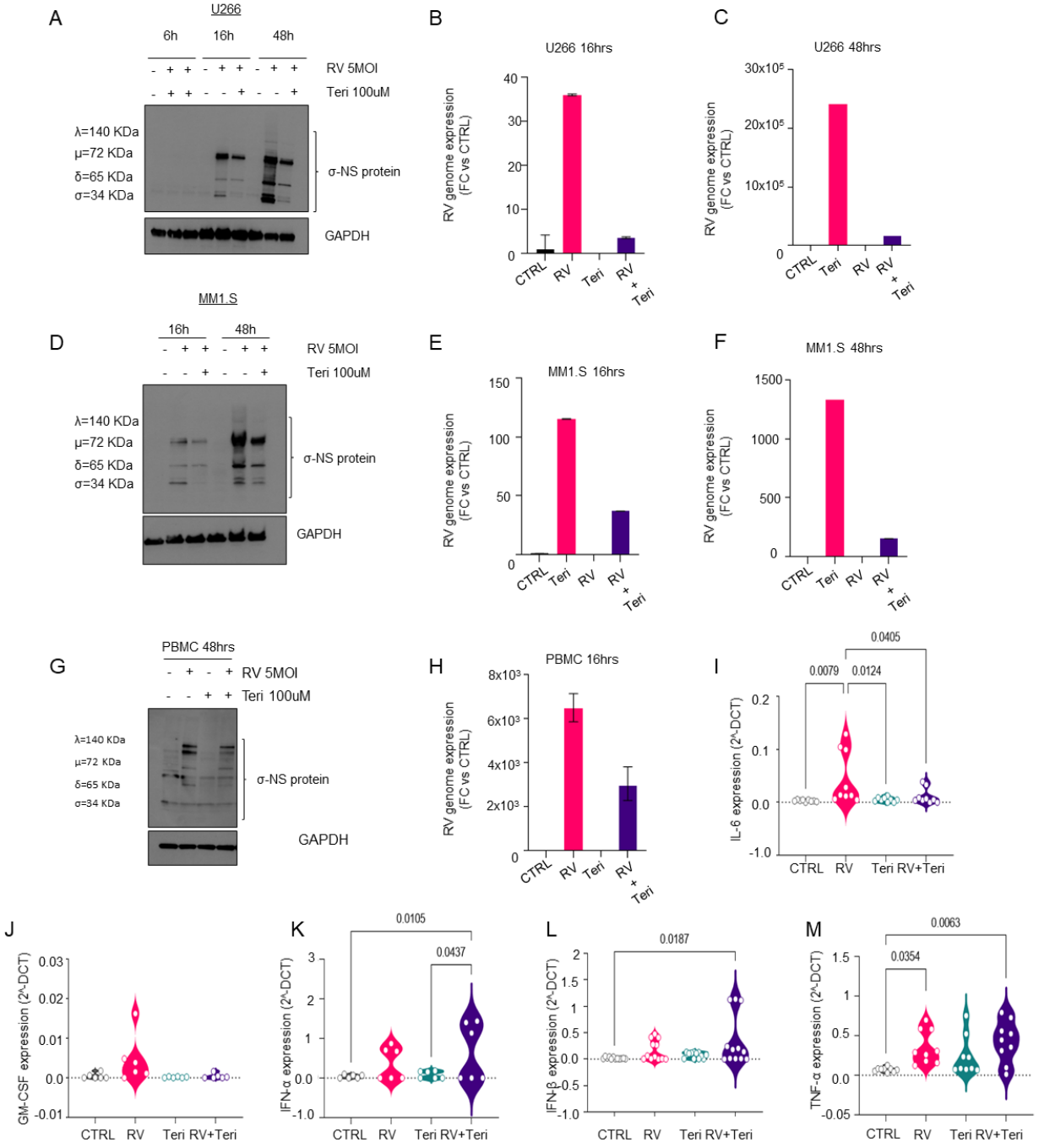

Supplementary Figure 1: A-B-C) Western Blot analysis of σ-NS viral protein in U266 cells after 6, 16 and 48hrs of treatment with teriflunomide (100 μm) and/or RV (5 MOI) infection (A), and q-RT-PCR for the viral genome expression after 16hrs (B) or 48hrs (C), normalized compared to control GAPDH and expressed as the mean ± SEM of triplicates in fold-change compared to the control; **D-E-F)** Western Blot analysis of σ-NS viral protein in MM1.S cells after 16 and 48hrs of treatment with teriflunomide (100 μm) and/or RV (5 MOI) infection (D), and q-RT-PCR for the viral genome expression after 16hrs (E) or 48hrs (F), normalized compared to control GAPDH and expressed as the mean ± SEM of triplicates in fold-change compared to the control; **G-H)** Western Blot analysis of (σ-NS) viral protein in healthy donor PBMC treated for 48hrs with teriflunomide (100 μM) and infected with RV (5 MOI); H) After 16hrs, RNA was isolated, and expression of the RV genome was determined by q-RT-PCR. Data were normalized compared to control GAPDH and expressed as the mean ± SEM of triplicates as fold-change compared to the control; **I-J-K-L-M)** PBMCs obtained from healthy donors were treated with teriflunomide (100 μM) and/or RV (5 MOI) and infected for 16hrs to assess the cytokine (IL-6, GM-CSF, IFN-α, IFN-β, TNF-α) mRNA expression profile by q-RT-PCR. For IL-6 and GM-CSF, data are expressed as the mean ± SEM (IL-6 and GM-CSF n=2 healthy donors; IFN-α, IFN-β and TNF-α n=3 healthy doors), normalized compared to control GAPDH; Comparisons among groups were performed by one-way ANOVA.

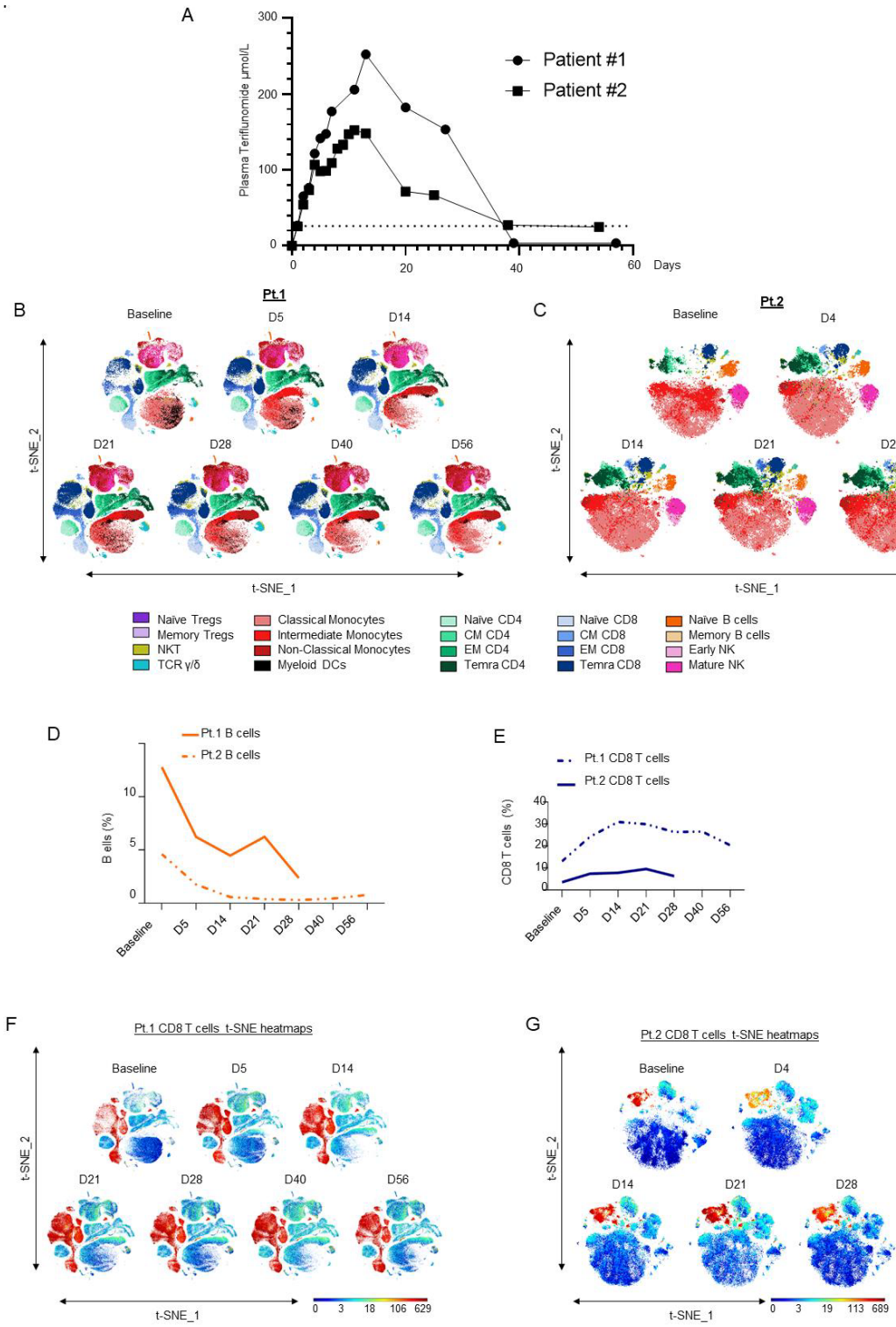

Supplementary Figure 2: A) Teriflunomide plasma concentration-versus-time plots for 2 patients receiving leflunomide. The dashed line represents the in vitro EC50 for teriflunomide against SARS-CoV-2 (26 µmol/L). **B-C)** In-depth longitudinal immune profiling of two patients with COVID-19 and breast cancer (A and B) treated with 40 mg leflunomide. A Maxpar Direct Immune Profiling System using a dry 30-marker antibody panel was employed. Hierarchical clustering and statistical mapping were performed algorithmically via the Cytobank© platform. vi-SNE analysis (iterations=1000, perplexity=100) are displayed in 2D plots using the resultant t-SNE 1 and t-SNE2 dimensions. High-fidelity FlowSOM ("self-organizing map") (metacluster=10 and cluster=100) based on vi-SNE 2D plots showing 20 different immune-compartments was used; **D)** Line graphs showing B cell expression as a percentage of the total PBMC population in Patients 1 and 2 as measured by CyTOF; **E)** Line graphs showing CD8+ T cell expression as a percentage of the total PBMC population in Patients 1 and 2 as measured by CyTOF; **F-G)** t-SNE heatmaps showing overall CD8+ T cell expression in both patients.

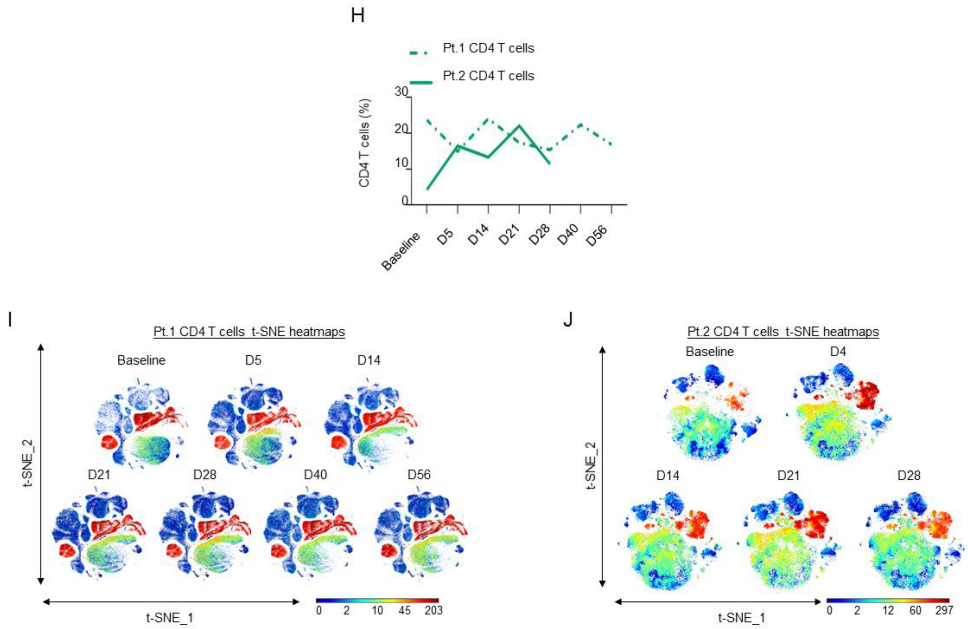

Supplementary Figure 2: H) Line graphs showing CD4+ T cell expression as a percentage of the total PBMC population in Patients 1 and 2 as measured by CyTOF; **I-J)** t-SNE heatmaps showing overall CD4+ T cell expression in both patients.

Supplemental Table 1: Maxpar direct immune profiling assay 30-marker panel with clones and heavy metals (Fluidigm)

Target	Clone	Metal
Anti-human CD45	HI30	89Y
Live/dead 103Rh-Intercalator (500 µM)	N/A	103Rh
Anti-human CD196/CCR6	G034E3	141Pr
Anti-human CD123	6H6	143Nd
Anti-human CD19	HIB19	144Nd
Anti-human CD4	RPA-T4	145Nd
Anti-human CD8a	RPA-T8	146Nd
Anti-human CD11c	Bu15	147Sm
Anti-human CD16	3G8	148Nd
Anti-human CD45RO	UCHL1	149Sm
Anti-human CD45RA	HI100	150Nd
Anti-human CD161	HP-3G10	151Eu
Anti-human CD194/CCR4	L291H4	152Sm
Anti-human CD25	BC96	153Eu
Anti-human CD27	O323	154Sm
Anti-human CD57	HCD57	155Gd
Anti-human CD183/CXCR3	G025H7	156Gd
Anti-human CD185/CXCR5	J252D4	158Gd
Anti-human CD28	CD28.2	160Gd
Anti-human CD38	HB-7	161Dy
Anti-human CD56/NCAM	NCAM16.2	163Dy
Anti-human TCRgd	B1	164Dy
Anti-human CD294	BM16	166Er
Anti-human CD197/CCR7	G043H7	167Er
Anti-human CD14	63D3	168Er
Anti-human CD3	UCHT1	170Er
Anti-human CD20	2H7	171Yb
Anti-human CD66b	G10F5	172Yb
Anti-human HLA-DR	LN3	173Yb
Anti-human IgD	IA6-2	174Yb
Anti-human CD127	A019D5	176Yb

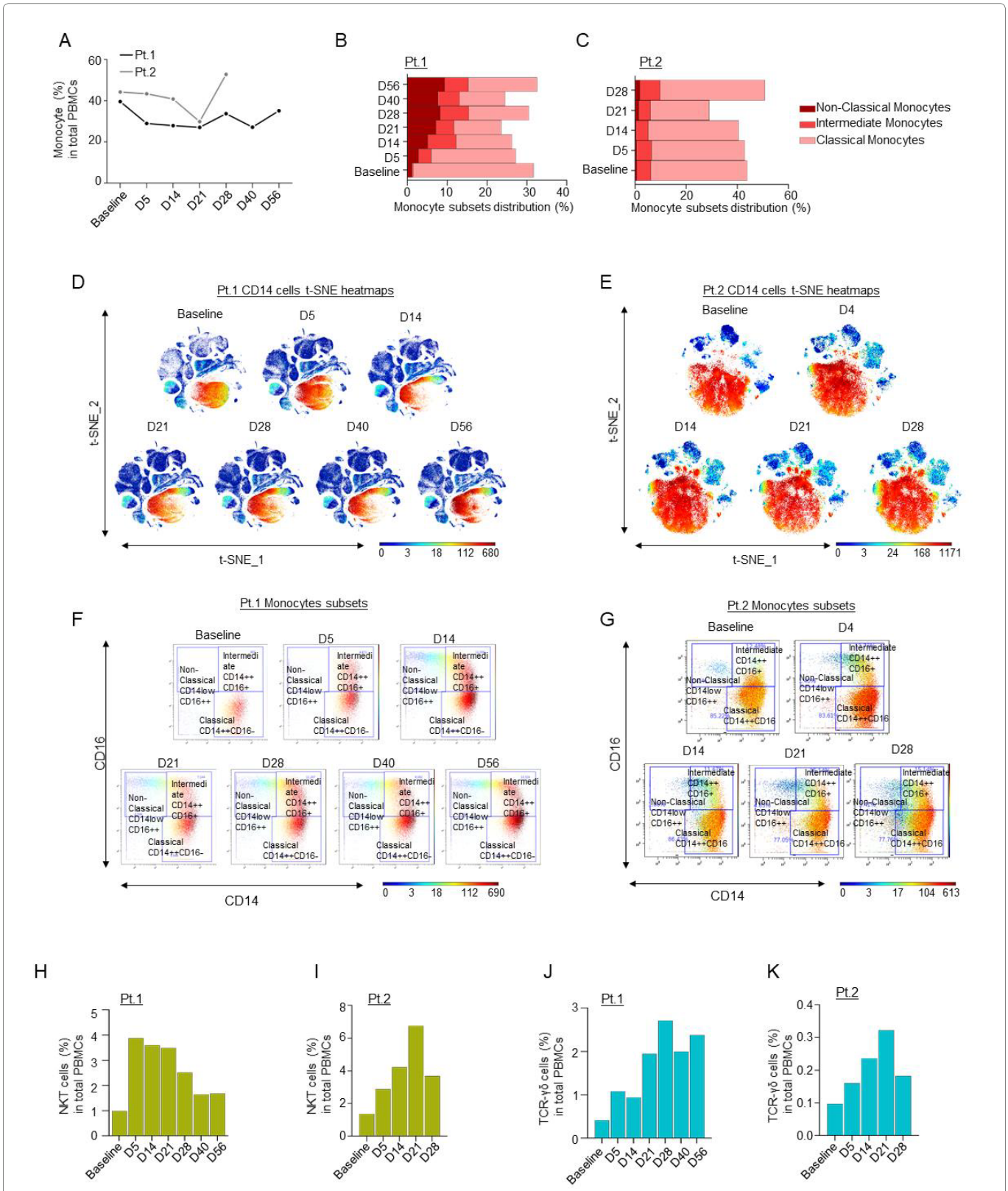

Supplementary Figure 3: A) Line graph showing percentages of monocyte cells in PBMCs in both patients; **B-C)** Bar graphs showing percentages of monocyte cell immune sub-compartments, based on CD14 and CD16 expression; **D-E)** t-SNE heatmaps showing overall CD14 expression through the course of treatment in patients 1 and 2; **F-G)** Dot plots colored by CD14 channel for the signal of Classical, Intermediate and Non-Classical monocyte expression through the course of treatment. **H-I)** Bar graphs showing percentages of NKT cells compared to the total count PBMCs in Patients 1 (H) and 2 (I) over time, as measured by CyTOF; **J-K)** Bar graphs showing percentages of TCR-γδ cells compared to the total count PBMC in Patients 1 (J) and 2 (K) over time, as measured by CyTOF.

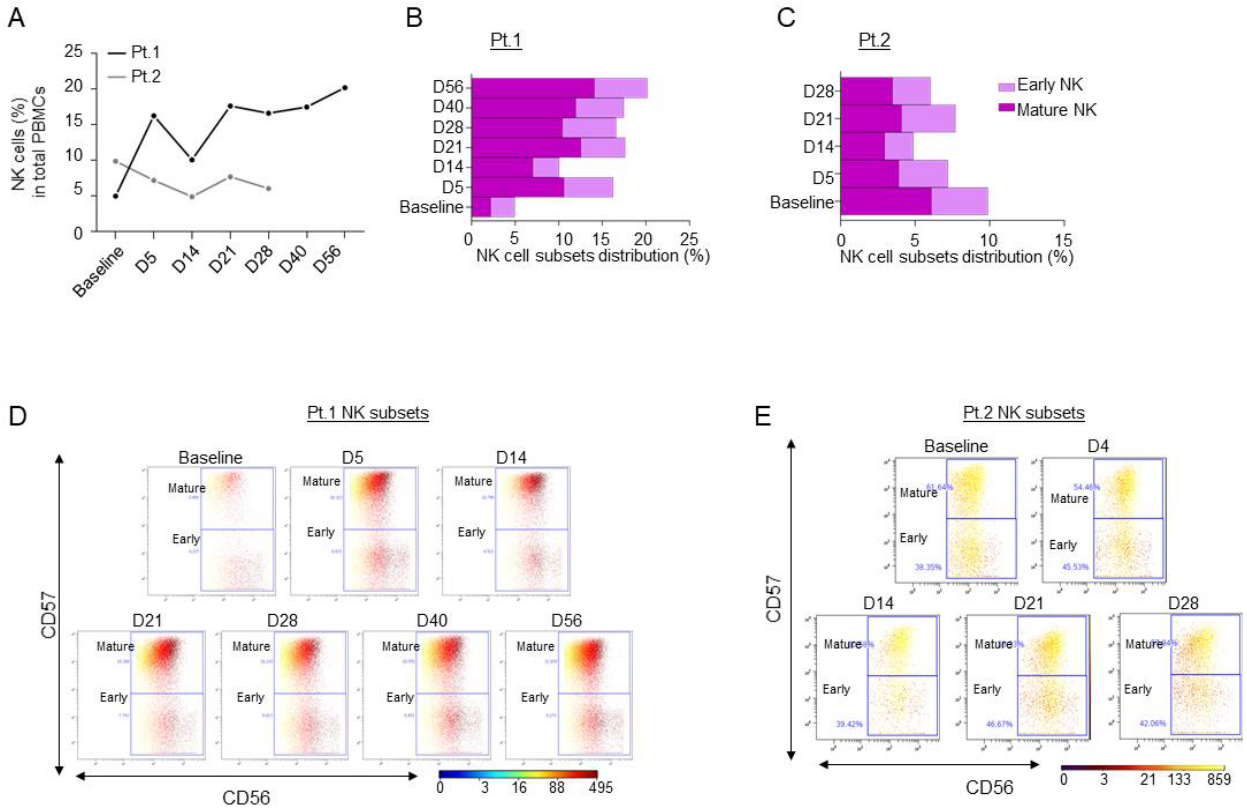

Supplementary Figure 4: A-B-C) Line graph showing percentages of NK cells in both patients (A), and bar graphs showing percentages of early and mature NK cell immune sub-compartments in both patients at the indicated timepoints (B-C); **D-E)** Dot plots colored by CD56 channel for the signal of early and mature NK cell expression through the course of treatment.

Supplemental Table 2. CyTOF gating strategy

Cell subsets	Model phenotypes
Naïve B-cells	CD45+ CD3- CD19+ CD20+ HLA-DR+ CD27-
Memory B-cells	CD45+ CD3- CD19+ CD20+ HLA-DR+ CD27+
Early NK	CD45+ CD3- CD19- CD14- CD56+ CD16-
Mature NK	CD45+ CD3- CD19- CD14- CD56+ CD16+
M-MDSCs	CD45+ CD3- CD19- CD11b+ CD33+ CD14+ HLA-DR-/dim
Classical Monos	CD45+ CD3- CD19- CD56- CD11b+ CD33+ HLA-DR+ CD14+ CD16-
Intermediate Monos	CD45+ CD3- CD19- CD56- CD11b+ CD33+ HLA-DR+ CD14+ CD16+
Non-Classical Monos	CD45+ CD3- CD19- CD56- CD11b+ CD33+ HLA-DR+ CD14- /dim CD16++
RV in Monos	CD45+ CD3- CD19- CD56- CD11b+ CD33+ HLA-DR+ CD14+ RV+
NKt-cells	CD45+ CD19- CD3+ CD56+
TCR γδ	CD45+ CD19- CD3+ CD56- TCRgd+
AE T-cells	CD45+ CD19- CD3+ CD56- TCRgd- CD8- CD4+ CD25+ CD127+
Memory Tregs	CD45+ CD19- CD3+ CD56- TCRgd- CD8- CD4+ CD25+ CD127low/- CD45RA-
Naïve Tregs	CD45+ CD19- CD3+ CD56- TCRgd- CD8- CD4+ CD25+ CD127low/- CD45RA+
CM CD8	CD45+ CD19- CD3+ CD56- TCRgd- CD8+ CD4- CD45RA- CCR7+ CD27+
EM CD8	CD45+ CD19- CD3+ CD56- TCRgd- CD8+ CD4- CD45RA- CCR7- CD27+
Naïve CD8	CD45+ CD19- CD3+ CD56- TCRgd- CD8+ CD4- CD45RA+ CCR7+ CD27+
TEMRA CD8	CD45+ CD19- CD3+ CD56- TCRgd- CD8+ CD4- CD45RA+ CCR7- CD27-
CM CD4	CD45+ CD19- CD3+ CD56- TCRgd- CD8- CD4+ CD25- CD127+CD45RA- CCR7+ CD27+
EM CD4	CD45+ CD19- CD3+ CD56- TCRgd- CD8- CD4+ CD25- CD127+CD45RA- CCR7- CD27+
Naïve CD4	CD45+ CD19- CD3+ CD56- TCRgd- CD8- CD4+ CD25- CD127+CD45RA+ CCR7+ CD27+
TEMRA CD4	CD45+ CD19- CD3+ CD56- TCRgd- CD8- CD4+ CD25- CD127+/dim CD45RA+ CCR7- CD27-

Supplemental Table 3. CyTOF counts, Patient 1

Timepoint	Population	FCS Filename	Event count
Baseline	Leukocytes	20291_PB_Basline	151061
Baseline	Granulocytes	20291_PB_Basline	0
Baseline	PBMCs	20291_PB_Basline	151061
Baseline	B-cells	20291_PB_Basline	6986
Baseline	Naive B-cells	20291_PB_Basline	4515
Baseline	Total Memory B-cells	20291_PB_Basline	2471
Baseline	Memory B-cells	20291_PB_Basline	246
Baseline	Plasmablast	20291_PB_Basline	2160
Baseline	CD3- CD19-	20291_PB_Basline	85407
Baseline	CD56+ CD14+	20291_PB_Basline	18060
Baseline	NK-cells	20291_PB_Basline	7512
Baseline	Early NK	20291_PB_Basline	4185
Baseline	Mature NK	20291_PB_Basline	3322
Baseline	Monocytes ?	20291_PB_Basline	59803
Baseline	Classical Monocytes	20291_PB_Basline	45571
Baseline	Intermediate Monocytes	20291_PB_Basline	412
Baseline	Non-Classical Monocytes	20291_PB_Basline	1858
Baseline	CD14- CD16-	20291_PB_Basline	11712
Baseline	Myeloid Dendritic cells	20291_PB_Basline	1604
Baseline	Plasmacytoid Dendritic cells	20291_PB_Basline	47
Baseline	CD3+	20291_PB_Basline	58560
Baseline	NKT	20291_PB_Basline	1486
Baseline	T-cells	20291_PB_Basline	57072
Baseline	TCR g/d	20291_PB_Basline	620
Baseline	TCR a/b	20291_PB_Basline	56452
Baseline	CD8 T-cells	20291_PB_Basline	19802
Baseline	Effector CD8 T-cells	20291_PB_Basline	1220
Baseline	Naive CD8	20291_PB_Basline	7996
Baseline	CD8+ CD27-	20291_PB_Basline	5143
Baseline	Late differentiated CD8 T-cells	20291_PB_Basline	1650
Baseline	Temra CD8	20291_PB_Basline	3488
Baseline	CD8+ CD45RA- CD27+	20291_PB_Basline	5450
Baseline	CM CD8	20291_PB_Basline	2317
Baseline	CD8+ CD45RA- CD27+ CCR7-	20291_PB_Basline	3123
Baseline	EM CD8	20291_PB_Basline	1253
Baseline	Transitional memory CD8 T-cells	20291_PB_Basline	1870
Baseline	CD4 T-cells	20291_PB_Basline	35741
Baseline	CD4+ CD25+	20291_PB_Basline	1649
Baseline	Activated Effector CD4 T-cells	20291_PB_Basline	319
Baseline	Total Tregs	20291_PB_Basline	1330
Baseline	Memory Tregs	20291_PB_Basline	1301
Baseline	Naive Tregs	20291_PB_Basline	29
Baseline	CD4+ CD25-	20291_PB_Basline	34092
Baseline	CM CD4 T-cells	20291_PB_Basline	16059
Baseline	Naive CD4 T-cells	20291_PB_Basline	10541
Baseline	CD4+ CCR7- CD45RA?	20291_PB_Basline	7473
Baseline	EM CD4	20291_PB_Basline	5353
Baseline	Temra CD4	20291_PB_Basline	2120
D5	Leukocytes	20291_PB_D5	151061
D5	Granulocytes	20291_PB_D5	0
D5	PBMCs	20291_PB_D5	151061
D5	B-cells	20291_PB_D5	2667
D5	Naive B-cells	20291_PB_D5	1766
D5	Total Memory B-cells	20291_PB_D5	901
D5	Memory B-cells	20291_PB_D5	250
D5	Plasmablast	20291_PB_D5	605
D5	CD3- CD19-	20291_PB_D5	80611
D5	CD56+ CD14+	20291_PB_D5	12229
D5	NK-cells	20291_PB_D5	24543
D5	Early NK	20291_PB_D5	8525
D5	Mature NK	20291_PB_D5	15992
D5	Monocytes ?	20291_PB_D5	43783
D5	Classical Monocytes	20291_PB_D5	32035
D5	Intermediate Monocytes	20291_PB_D5	4817
D5	Non-Classical Monocytes	20291_PB_D5	4244
D5	CD14- CD16-	20291_PB_D5	2628
D5	Myeloid Dendritic cells	20291_PB_D5	547
D5	Plasmacytoid Dendritic cells	20291_PB_D5	31
D5	CD3+	20291_PB_D5	67731
D5	NKT	20291_PB_D5	5856
D5	T-cells	20291_PB_D5	61874
D5	TCR g/d	20291_PB_D5	1629
D5	TCR a/b	20291_PB_D5	60245
D5	CD8 T-cells	20291_PB_D5	36652
D5	Effector CD8 T-cells	20291_PB_D5	4553
D5	Naive CD8	20291_PB_D5	5435
D5	CD8+ CD27-	20291_PB_D5	21065
D5	Late differentiated CD8 T-cells	20291_PB_D5	5815
D5	Temra CD8	20291_PB_D5	15243
D5	CD8+ CD45RA- CD27+	20291_PB_D5	5613
D5	CM CD8	20291_PB_D5	1273
D5	CD8+ CD45RA- CD27+ CCR7-	20291_PB_D5	4334
D5	EM CD8	20291_PB_D5	2579
D5	Transitional memory CD8 T-cells	20291_PB_D5	1755
D5	CD4 T-cells	20291_PB_D5	22510
D5	CD4+ CD25+	20291_PB_D5	856
D5	Activated Effector CD4 T-cells	20291_PB_D5	228
D5	Total Tregs	20291_PB_D5	628
D5	Memory Tregs	20291_PB_D5	617
D5	Naive Tregs	20291_PB_D5	11
D5	CD4+ CD25-	20291_PB_D5	21654
D5	CM CD4 T-cells	20291_PB_D5	8378
D5	Naive CD4 T-cells	20291_PB_D5	5390
D5	CD4+ CCR7- CD45RA?	20291_PB_D5	7874
D5	EM CD4	20291_PB_D5	4788
D5	Temra CD4	20291_PB_D5	3086

D8	Leukocytes	20291_PB_D8	151061
D8	Granulocytes	20291_PB_D8	0
D8	PBMCs	20291_PB_D8	151061
D8	B-cells	20291_PB_D8	2670
D8	Naive B-cells	20291_PB_D8	2093
D8	Total Memory B-cells	20291_PB_D8	577
D8	Memory B-cells	20291_PB_D8	384
D8	Plasmablast	20291_PB_D8	154
D8	CD3- CD19-	20291_PB_D8	76613
D8	CD56+ CD14+	20291_PB_D8	14437
D8	NK-cells	20291_PB_D8	12448
D8	Early NK	20291_PB_D8	4902
D8	Mature NK	20291_PB_D8	7536
D8	Monocytes ?	20291_PB_D8	49677
D8	Classical Monocytes	20291_PB_D8	40484
D8	Intermediate Monocytes	20291_PB_D8	1687
D8	Non-Classical Monocytes	20291_PB_D8	2666
D8	CD14- CD16-	20291_PB_D8	4737
D8	Myeloid Dendritic cells	20291_PB_D8	576
D8	Plasmacytoid Dendritic cells	20291_PB_D8	75
D8	CD3+	20291_PB_D8	71737
D8	NKT	20291_PB_D8	4110
D8	T-cells	20291_PB_D8	67625
D8	TCR g/d	20291_PB_D8	1291
D8	TCR a/b	20291_PB_D8	66334
D8	CD8 T-cells	20291_PB_D8	30916
D8	Effector CD8 T-cells	20291_PB_D8	3711
D8	Naive CD8	20291_PB_D8	6102
D8	CD8+ CD27-	20291_PB_D8	12227
D8	Late differentiated CD8 T-cells	20291_PB_D8	3473
D8	Temra CD8	20291_PB_D8	8754
D8	CD8+ CD45RA- CD27+	20291_PB_D8	8882
D8	CM CD8	20291_PB_D8	3057
D8	CD8+ CD45RA- CD27+ CCR7-	20291_PB_D8	5814
D8	EM CD8	20291_PB_D8	2298
D8	Transitional memory CD8 T-cells	20291_PB_D8	3516
D8	CD4 T-cells	20291_PB_D8	34085
D8	CD4+ CD25+	20291_PB_D8	1257
D8	Activated Effector CD4 T-cells	20291_PB_D8	285
D8	Total Tregs	20291_PB_D8	972
D8	Memory Tregs	20291_PB_D8	958
D8	Naive Tregs	20291_PB_D8	14
D8	CD4+ CD25-	20291_PB_D8	32828
D8	CM CD4 T-cells	20291_PB_D8	15459
D8	Naive CD4 T-cells	20291_PB_D8	5126
D8	CD4+ CCR7- CD45RA?	20291_PB_D8	12220
D8	EM CD4	20291_PB_D8	8907
D8	Temra CD4	20291_PB_D8	3313
D14	Leukocytes	20291_PB_D14	151061
D14	Granulocytes	20291_PB_D14	0
D14	PBMCs	20291_PB_D14	151061
D14	B-cells	20291_PB_D14	897
D14	Naive B-cells	20291_PB_D14	765
D14	Total Memory B-cells	20291_PB_D14	132
D14	Memory B-cells	20291_PB_D14	104
D14	Plasmablast	20291_PB_D14	26
D14	CD3- CD19-	20291_PB_D14	58555
D14	CD56+ CD14+	20291_PB_D14	1185
D14	NK-cells	20291_PB_D14	15179
D14	Early NK	20291_PB_D14	4511
D14	Mature NK	20291_PB_D14	10650
D14	Monocytes ?	20291_PB_D14	42158
D14	Classical Monocytes	20291_PB_D14	21098
D14	Intermediate Monocytes	20291_PB_D14	10818
D14	Non-Classical Monocytes	20291_PB_D14	7742
D14	CD14- CD16-	20291_PB_D14	2534
D14	Myeloid Dendritic cells	20291_PB_D14	1199
D14	Plasmacytoid Dendritic cells	20291_PB_D14	800
D14	CD3+	20291_PB_D14	91559
D14	NKT	20291_PB_D14	5436
D14	T-cells	20291_PB_D14	86108
D14	TCR g/d	20291_PB_D14	1418
D14	TCR a/b	20291_PB_D14	84690
D14	CD8 T-cells	20291_PB_D14	46721
D14	Effector CD8 T-cells	20291_PB_D14	6100
D14	Naive CD8	20291_PB_D14	8287
D14	CD8+ CD27-	20291_PB_D14	17649
D14	Late differentiated CD8 T-cells	20291_PB_D14	4910
D14	Temra CD8	20291_PB_D14	12739
D14	CD8+ CD45RA- CD27+	20291_PB_D14	14706
D14	CM CD8	20291_PB_D14	3339
D14	CD8+ CD45RA- CD27+ CCR7-	20291_PB_D14	11354
D14	EM CD8	20291_PB_D14	5743
D14	Transitional memory CD8 T-cells	20291_PB_D14	5611
D14	CD4 T-cells	20291_PB_D14	36245
D14	CD4+ CD25+	20291_PB_D14	1234
D14	Activated Effector CD4 T-cells	20291_PB_D14	165
D14	Total Tregs	20291_PB_D14	1069
D14	Memory Tregs	20291_PB_D14	939
D14	Naive Tregs	20291_PB_D14	130
D14	CD4+ CD25-	20291_PB_D14	35011
D14	CM CD4 T-cells	20291_PB_D14	16288
D14	Naive CD4 T-cells	20291_PB_D14	10797
D14	CD4+ CCR7- CD45RA?	20291_PB_D14	7899
D14	EM CD4	20291_PB_D14	4888
D14	Temra CD4	20291_PB_D14	3011
D21	Leukocytes	20291_PB_D21	151061
D21	Granulocytes	20291_PB_D21	0
D21	PBMCs	20291_PB_D21	151061
D21	B-cells	20291_PB_D21	607

D21	Naive B-cells	20291_PB_D21	564
D21	Total Memory B-cells	20291_PB_D21	43
D21	Memory B-cells	20291_PB_D21	37
D21	Plasmablast	20291_PB_D21	4
D21	CD3- CD19-	20291_PB_D21	68944
D21	CD56+ CD14+	20291_PB_D21	1396
D21	NK-cells	20291_PB_D21	26605
D21	Early NK	20291_PB_D21	7638
D21	Mature NK	20291_PB_D21	18946
D21	Monocytes ?	20291_PB_D21	40864
D21	Classical Monocytes	20291_PB_D21	17955
D21	Intermediate Monocytes	20291_PB_D21	6880
D21	Non-Classical Monocytes	20291_PB_D21	10871
D21	CD14- CD16-	20291_PB_D21	5147
D21	Myeloid Dendritic cells	20291_PB_D21	1701
D21	Plasmacytoid Dendritic cells	20291_PB_D21	1644
D21	CD3+	20291_PB_D21	81442
D21	NKT	20291_PB_D21	5272
D21	T-cells	20291_PB_D21	76163
D21	TCR g/d	20291_PB_D21	2945
D21	TCR a/b	20291_PB_D21	73218
D21	CD8 T-cells	20291_PB_D21	45223
D21	Effector CD8 T-cells	20291_PB_D21	10028
D21	Naive CD8	20291_PB_D21	5742
D21	CD8+ CD27-	20291_PB_D21	18462
D21	Late differentiated CD8 T-cells	20291_PB_D21	5045
D21	Temra CD8	20291_PB_D21	13414
D21	CD8+ CD45RA- CD27+	20291_PB_D21	11026
D21	CM CD8	20291_PB_D21	1706
D21	CD8+ CD45RA- CD27+ CCR7-	20291_PB_D21	9310
D21	EM CD8	20291_PB_D21	6616
D21	Transitional memory CD8 T-cells	20291_PB_D21	2694
D21	CD4 T-cells	20291_PB_D21	26209
D21	CD4+ CD25+	20291_PB_D21	1477
D21	Activated Effector CD4 T-cells	20291_PB_D21	206
D21	Total Tregs	20291_PB_D21	1271
D21	Memory Tregs	20291_PB_D21	1168
D21	Naive Tregs	20291_PB_D21	103
D21	CD4+ CD25-	20291_PB_D21	24732
D21	CM CD4 T-cells	20291_PB_D21	8595
D21	Naive CD4 T-cells	20291_PB_D21	6552
D21	CD4+ CCR7- CD45RA?	20291_PB_D21	9574
D21	EM CD4	20291_PB_D21	3545
D21	Temra CD4	20291_PB_D21	6029
D28	Leukocytes	20291_PB_D28	151061
D28	Granulocytes	20291_PB_D28	0
D28	PBMCs	20291_PB_D28	151061
D28	B-cells	20291_PB_D28	476
D28	Naive B-cells	20291_PB_D28	448
D28	Total Memory B-cells	20291_PB_D28	28
D28	Memory B-cells	20291_PB_D28	21
D28	Plasmablast	20291_PB_D28	7
D28	CD3- CD19-	20291_PB_D28	77699
D28	CD56+ CD14+	20291_PB_D28	1618
D28	NK-cells	20291_PB_D28	25055
D28	Early NK	20291_PB_D28	9258
D28	Mature NK	20291_PB_D28	15773
D28	Monocytes ?	20291_PB_D28	50952
D28	Classical Monocytes	20291_PB_D28	22859
D28	Intermediate Monocytes	20291_PB_D28	10833
D28	Non-Classical Monocytes	20291_PB_D28	12452
D28	CD14- CD16-	20291_PB_D28	4828
D28	Myeloid Dendritic cells	20291_PB_D28	1566
D28	Plasmacytoid Dendritic cells	20291_PB_D28	1749
D28	CD3+	20291_PB_D28	72834
D28	NKT	20291_PB_D28	3806
D28	T-cells	20291_PB_D28	69023
D28	TCR g/d	20291_PB_D28	4092
D28	TCR a/b	20291_PB_D28	64931
D28	CD8 T-cells	20291_PB_D28	39848
D28	Effector CD8 T-cells	20291_PB_D28	12908
D28	Naive CD8	20291_PB_D28	4526
D28	CD8+ CD27-	20291_PB_D28	14265
D28	Late differentiated CD8 T-cells	20291_PB_D28	4261
D28	Temra CD8	20291_PB_D28	10004
D28	CD8+ CD45RA- CD27+	20291_PB_D28	8160
D28	CM CD8	20291_PB_D28	1624
D28	CD8+ CD45RA- CD27+ CCR7-	20291_PB_D28	6524
D28	EM CD8	20291_PB_D28	4572
D28	Transitional memory CD8 T-cells	20291_PB_D28	1952
D28	CD4 T-cells	20291_PB_D28	23246
D28	CD4+ CD25+	20291_PB_D28	1010
D28	Activated Effector CD4 T-cells	20291_PB_D28	128
D28	Total Tregs	20291_PB_D28	882
D28	Memory Tregs	20291_PB_D28	835
D28	Naive Tregs	20291_PB_D28	47
D28	CD4+ CD25-	20291_PB_D28	22236
D28	CM CD4 T-cells	20291_PB_D28	8490
D28	Naive CD4 T-cells	20291_PB_D28	5365
D28	CD4+ CCR7- CD45RA?	20291_PB_D28	8371
D28	EM CD4	20291_PB_D28	3362
D28	Temra CD4	20291_PB_D28	5009
D40	Leukocytes	20291_PB_D40	151061
D40	Granulocytes	20291_PB_D40	0
D40	PBMCs	20291_PB_D40	151061
D40	B-cells	20291_PB_D40	689
D40	Naive B-cells	20291_PB_D40	425
D40	Total Memory B-cells	20291_PB_D40	264
D40	Memory B-cells	20291_PB_D40	38
D40	Plasmablast	20291_PB_D40	206

D40	CD3- CD19-	20291_PB_D40	69036
D40	CD56+ CD14+	20291_PB_D40	1481
D40	NK-cells	20291_PB_D40	26394
D40	Early NK	20291_PB_D40	8310
D40	Mature NK	20291_PB_D40	18050
D40	Monocytes ?	20291_PB_D40	41087
D40	Classical Monocytes	20291_PB_D40	17194
D40	Intermediate Monocytes	20291_PB_D40	8146
D40	Non-Classical Monocytes	20291_PB_D40	11709
D40	CD14- CD16-	20291_PB_D40	4072
D40	Myeloid Dendritic cells	20291_PB_D40	1331
D40	Plasmacytoid Dendritic cells	20291_PB_D40	644
D40	CD3+	20291_PB_D40	81280
D40	NKT	20291_PB_D40	2476
D40	T-cells	20291_PB_D40	78802
D40	TCR g/d	20291_PB_D40	3016
D40	TCR a/b	20291_PB_D40	75786
D40	CD8 T-cells	20291_PB_D40	40159
D40	Effector CD8 T-cells	20291_PB_D40	10555
D40	Naive CD8	20291_PB_D40	6122
D40	CD8+ CD27-	20291_PB_D40	14136
D40	Late differentiated CD8 T-cells	20291_PB_D40	3103
D40	Temra CD8	20291_PB_D40	11015
D40	CD8+ CD45RA- CD27+	20291_PB_D40	9392
D40	CM CD8	20291_PB_D40	2300
D40	CD8+ CD45RA- CD27+ CCR7-	20291_PB_D40	7082
D40	EM CD8	20291_PB_D40	4816
D40	Transitional memory CD8 T-cells	20291_PB_D40	2266
D40	CD4 T-cells	20291_PB_D40	33775
D40	CD4+ CD25+	20291_PB_D40	952
D40	Activated Effector CD4 T-cells	20291_PB_D40	134
D40	Total Tregs	20291_PB_D40	818
D40	Memory Tregs	20291_PB_D40	749
D40	Naive Tregs	20291_PB_D40	69
D40	CD4+ CD25-	20291_PB_D40	32823
D40	CM CD4 T-cells	20291_PB_D40	12546
D40	Naive CD4 T-cells	20291_PB_D40	7278
D40	CD4+ CCR7- CD45RA?	20291_PB_D40	12963
D40	EM CD4	20291_PB_D40	7191
D40	Temra CD4	20291_PB_D40	5772
D56	Leukocytes	20291_PB_D56	151061
D56	Granulocytes	20291_PB_D56	0
D56	PBMCs	20291_PB_D56	151061
D56	B-cells	20291_PB_D56	1205
D56	Naive B-cells	20291_PB_D56	805
D56	Total Memory B-cells	20291_PB_D56	400
D56	Memory B-cells	20291_PB_D56	66
D56	Plasmablast	20291_PB_D56	292
D56	CD3- CD19-	20291_PB_D56	85540
D56	CD56+ CD14+	20291_PB_D56	1927
D56	NK-cells	20291_PB_D56	30493
D56	Early NK	20291_PB_D56	9146
D56	Mature NK	20291_PB_D56	21311
D56	Monocytes ?	20291_PB_D56	53028
D56	Classical Monocytes	20291_PB_D56	26053
D56	Intermediate Monocytes	20291_PB_D56	8935
D56	Non-Classical Monocytes	20291_PB_D56	14216
D56	CD14- CD16-	20291_PB_D56	3861
D56	Myeloid Dendritic cells	20291_PB_D56	1022
D56	Plasmacytoid Dendritic cells	20291_PB_D56	1979
D56	CD3+	20291_PB_D56	64265
D56	NKT	20291_PB_D56	2541
D56	T-cells	20291_PB_D56	61720
D56	TCR g/d	20291_PB_D56	3596
D56	TCR a/b	20291_PB_D56	58124
D56	CD8 T-cells	20291_PB_D56	30821
D56	Effector CD8 T-cells	20291_PB_D56	7494
D56	Naive CD8	20291_PB_D56	7316
D56	CD8+ CD27-	20291_PB_D56	10681
D56	Late differentiated CD8 T-cells	20291_PB_D56	2670
D56	Temra CD8	20291_PB_D56	8011
D56	CD8+ CD45RA- CD27+	20291_PB_D56	5350
D56	CM CD8	20291_PB_D56	1911
D56	CD8+ CD45RA- CD27+ CCR7-	20291_PB_D56	3430
D56	EM CD8	20291_PB_D56	2230
D56	Transitional memory CD8 T-cells	20291_PB_D56	1200
D56	CD4 T-cells	20291_PB_D56	25412
D56	CD4+ CD25+	20291_PB_D56	1293
D56	Activated Effector CD4 T-cells	20291_PB_D56	114
D56	Total Tregs	20291_PB_D56	1179
D56	Memory Tregs	20291_PB_D56	1084
D56	Naive Tregs	20291_PB_D56	95
D56	CD4+ CD25-	20291_PB_D56	24119
D56	CM CD4 T-cells	20291_PB_D56	8984
D56	Naive CD4 T-cells	20291_PB_D56	8027
D56	CD4+ CCR7- CD45RA?	20291_PB_D56	7095
D56	EM CD4	20291_PB_D56	3532
D56	Temra CD4	20291_PB_D56	3563

Supplemental Table 4. CyTOF Counts, Patient 2

Population	Timepoint	FCS Filename	Event count
PBMCs	Screening	Pt#2_Screening_PBMC_IRB20291_MDPA_11-10-2021_1_concat	95678
PBMCs	D4	Pt.#2_D4_PBMC_IRB20291_MDIPA_10-13-2021_1	95678
PBMCs	D8	Pt2_D8_PBMC_merge1	95678
PBMCs	D14	Pt.#2_D14_PBMC_IRB20291_MDIPA_10-13-2021_1	95678
PBMCs	D21	Pt.#2_D21_PBMC_IRB20291_MDIPA_10-13-2021_1	95678
PBMCs	D28	Pt.#2_D28_PBMC_IRB20291_MDIPA_10-13-2021_1	95678
B-cells	Screening	Pt#2_Screening_PBMC_IRB20291_MDPA_11-10-2021_1_concat	12212
B-cells	D4	Pt.#2_D4_PBMC_IRB20291_MDIPA_10-13-2021_1	5966
B-cells	D8	Pt2_D8_PBMC_merge1	3561
B-cells	D14	Pt.#2_D14_PBMC_IRB20291_MDIPA_10-13-2021_1	4293
B-cells	D21	Pt.#2_D21_PBMC_IRB20291_MDIPA_10-13-2021_1	5977
B-cells	D28	Pt.#2_D28_PBMC_IRB20291_MDIPA_10-13-2021_1	2283
Naive B-cells	Screening	Pt#2_Screening_PBMC_IRB20291_MDPA_11-10-2021_1_concat	12020
Naive B-cells	D4	Pt.#2_D4_PBMC_IRB20291_MDIPA_10-13-2021_1	5661
Naive B-cells	D8	Pt2_D8_PBMC_merge1	3528
Naive B-cells	D14	Pt.#2_D14_PBMC_IRB20291_MDIPA_10-13-2021_1	3865
Naive B-cells	D21	Pt.#2_D21_PBMC_IRB20291_MDIPA_10-13-2021_1	5140
Naive B-cells	D28	Pt.#2_D28_PBMC_IRB20291_MDIPA_10-13-2021_1	2232
Total Memory B-cells	Screening	Pt#2_Screening_PBMC_IRB20291_MDPA_11-10-2021_1_concat	191
Total Memory B-cells	D4	Pt.#2_D4_PBMC_IRB20291_MDIPA_10-13-2021_1	305
Total Memory B-cells	D8	Pt2_D8_PBMC_merge1	32
Total Memory B-cells	D14	Pt.#2_D14_PBMC_IRB20291_MDIPA_10-13-2021_1	427
Total Memory B-cells	D21	Pt.#2_D21_PBMC_IRB20291_MDIPA_10-13-2021_1	835
Total Memory B-cells	D28	Pt.#2_D28_PBMC_IRB20291_MDIPA_10-13-2021_1	51
Plasmablast	Screening	Pt#2_Screening_PBMC_IRB20291_MDPA_11-10-2021_1_concat	47
Plasmablast	D4	Pt.#2_D4_PBMC_IRB20291_MDIPA_10-13-2021_1	5
Plasmablast	D8	Pt2_D8_PBMC_merge1	4
Plasmablast	D14	Pt.#2_D14_PBMC_IRB20291_MDIPA_10-13-2021_1	8
Plasmablast	D21	Pt.#2_D21_PBMC_IRB20291_MDIPA_10-13-2021_1	23
Plasmablast	D28	Pt.#2_D28_PBMC_IRB20291_MDIPA_10-13-2021_1	7
NK-cells	Screening	Pt#2_Screening_PBMC_IRB20291_MDPA_11-10-2021_1_concat	9448
NK-cells	D4	Pt.#2_D4_PBMC_IRB20291_MDIPA_10-13-2021_1	6875
NK-cells	D8	Pt2_D8_PBMC_merge1	11434
NK-cells	D14	Pt.#2_D14_PBMC_IRB20291_MDIPA_10-13-2021_1	4670
NK-cells	D21	Pt.#2_D21_PBMC_IRB20291_MDIPA_10-13-2021_1	7353
NK-cells	D28	Pt.#2_D28_PBMC_IRB20291_MDIPA_10-13-2021_1	5770
Early NK	Screening	Pt#2_Screening_PBMC_IRB20291_MDPA_11-10-2021_1_concat	3623
Early NK	D4	Pt.#2_D4_PBMC_IRB20291_MDIPA_10-13-2021_1	3130
Early NK	D8	Pt2_D8_PBMC_merge1	4462
Early NK	D14	Pt.#2_D14_PBMC_IRB20291_MDIPA_10-13-2021_1	1841

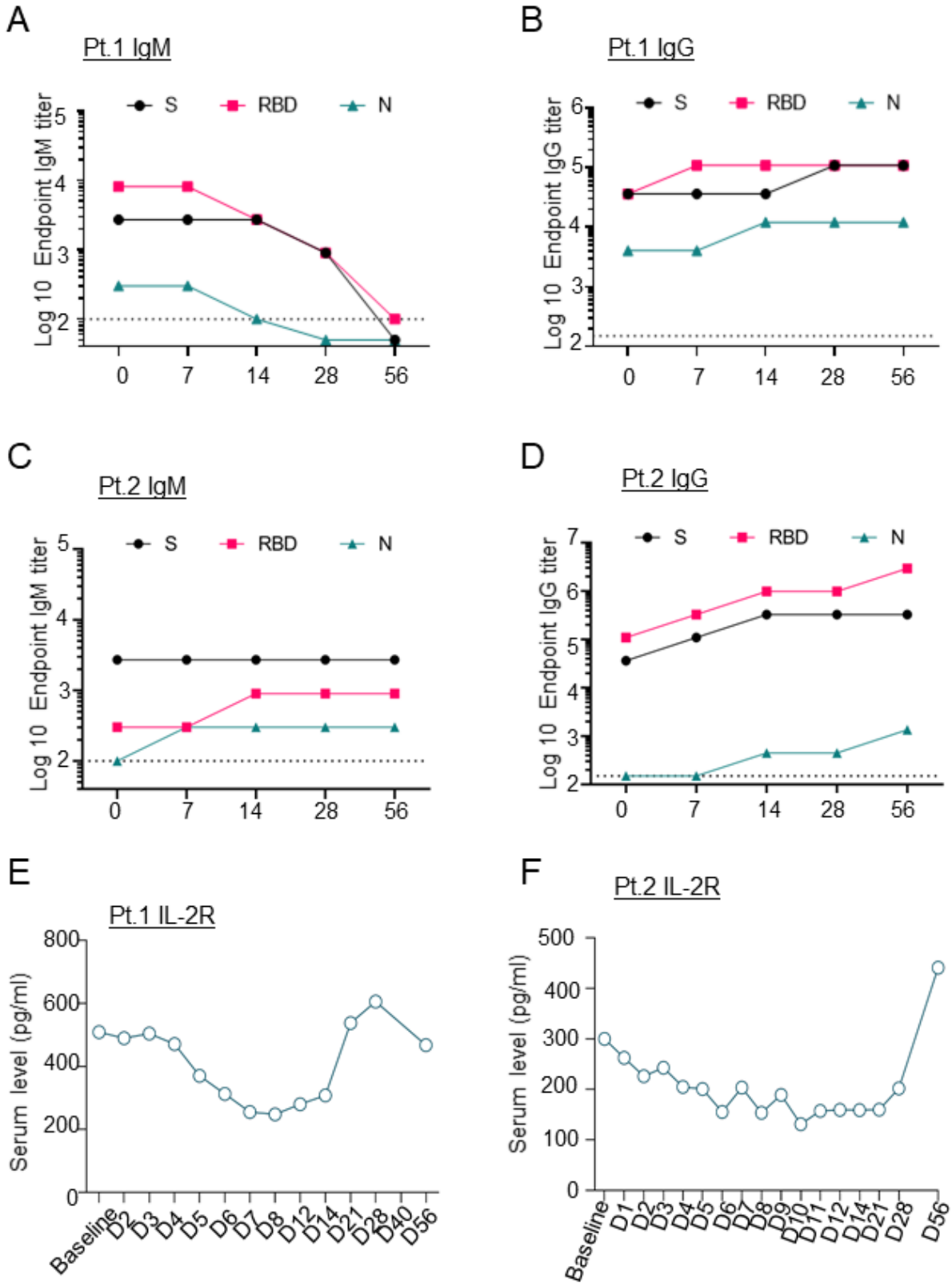

Supplementary Figure 5: A-B-C-D) Longitudinal evaluation of serum IgM (A,C) and IgG (B,D) immunoglobulin reactive to SARS-CoV-2 nucleoprotein (N), receptor-binding domain (RBD), and spike (S) collected from the patients at baseline (time zero), through the course of leflunomide treatment (up to 14 days) and follow up (up to 56 days); **E-F**) Longitudinal evaluation of serum cytokines IL-2R through the treatment course (14 days) and follow up appointments (up to day 56).